Towards a Second Generation SIS Receiver for ALMA Band 6

A. R. Kerr, J. Effland, A. W. Lichtenberger, and J. Mangum
NRAO
23 March 2016

Summary: This report describes work done towards a new generation of receivers for ALMA Band 6. While this work is focused on Band 6, much of it could be applied to all eight of the ALMA bands which use SIS receivers, namely Bands 3-10. Two aspects of the current Band-6 receivers can be improved: the receiver noise temperature can be made flatter across the RF and IF bands, and the gain variation across the IF band can be reduced. The eventual goal is to have relatively flat noise temperature and gain across the full 211-275 GHz Band 6 and across a full 4-12 GHz IF band. Three possible approaches are being studied: (i) the configuration of the front-end; (ii) the use of balanced IF preamplifiers; and (iii) SIS mixers with a wider RF bandwidth.

1. Front-end configuration

Several configurations are possible for receivers using sideband-separating and balanced mixers, and this section considers the relative merits of these. Sideband-separating mixers are used on ALMA Bands 3-8 as a means of reducing the atmospheric contribution to the system noise, but LO sideband noise also contributes a significant component of the system noise at some LO and intermediate frequencies, and this can potentially be reduced by using a balanced mixer configuration. Here, the input characteristics of balanced and sideband-separating mixers with quadrature and 180° input hybrids are examined. Like the balanced amplifier, balanced and sideband-separating mixers using a quadrature input hybrid are inherently well matched.

The levels of the signals emerging from the input port at the image and LO frequencies are also important in some applications, as are the down-converted local oscillator sideband noise and the thermal noise contribution of the fourth-port termination on the input hybrid. These depend on the mixer configuration. These effects are considered for balanced and sideband-separating mixers of the four basic types depicted in Figs. 1-4. All have input hybrids, either quadrature or 180°. Quadrature hybrids can be of the coupled transmission line or branch-line types, and 180° hybrids can use a magic-T, Wilkinson power divider, rat-race, or a simple transformer. In practice, 0° or 180° three-port power splitters are sometimes used in place of 180° hybrids, but these can lead to degradation of mixer performance due to reflection of even- or odd-mode signal components which would be terminated in the fourth-port load of a full four-port hybrid.

The analysis of these configurations is complex and is relegated to Appendix 1, but the results are summarized in Table 1.

TABLE 1 – COMPARISON OF TYPES OF BALANCED AND SIDEBAND-SEPARATING MIXERS

Type of mixer	Balanced		Sideband-separating	
Input hybrid type	**90°**	**180°**	**90°**	**180°**
Input matched	yes	no	yes	no
Signal-to-image conversion isolated from input	yes	no	no	yes
LO leakage isolated from input	no	yes	no	no
LO sideband noise isolated from mixer output	yes	yes	no	no
Noise from input hybrid termination isolated from mixer output	yes	yes	no	no
Noise from LO hybrid termination isolated from mixer output	no*	no*	no*	no*

* Noise from the fourth-port termination on the LO hybrid is attenuated by the LO coupler.

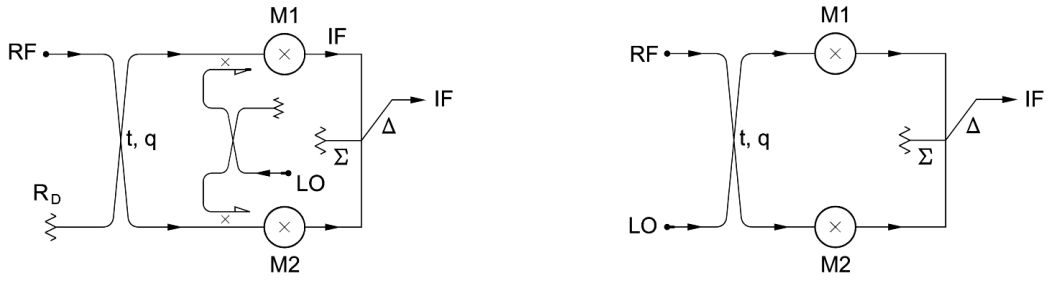

Fig. 1. Balanced mixer with a quadrature hybrid at its input. (a) Basic configuration. (b) The more common version in which the input hybrid is shared by the signal and LO.

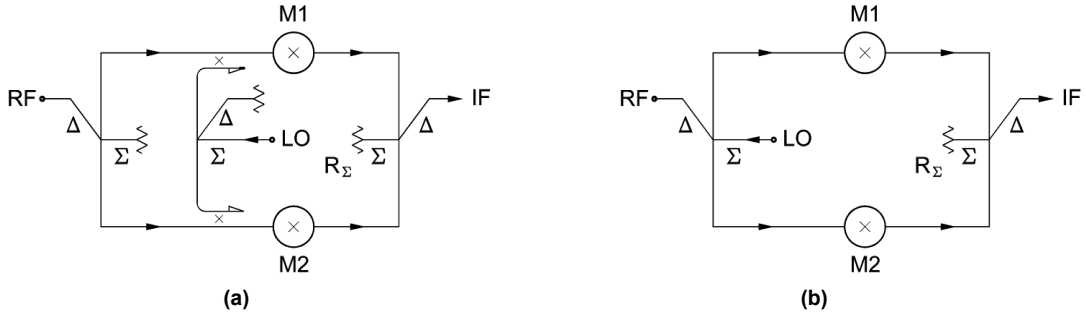

Fig. 2. Balanced mixer with a 180° hybrid at its input.(a) Basic configuration. (b) The more common version in which the input hybrid is shared by the signal and LO.

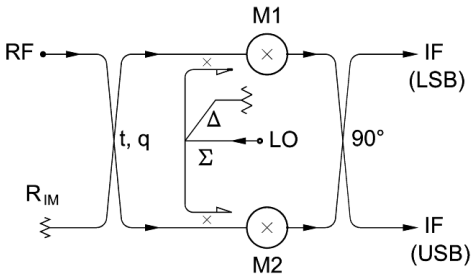

Fig. 3. Sideband-separating mixer with a quadrature hybrid at its input.

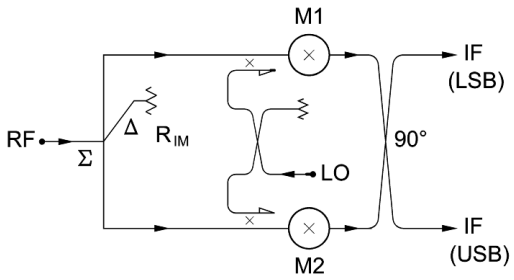

Fig. 4. Sideband-separating mixer with a 180° hybrid at its input.

Conclusions from Table 1:

The front-end configuration currently used in ALMA Bands 3-8 uses a 90° input hybrid, as shown in Fig. 3. This has an inherently well matched RF input, which is important for minimizing baseline ripples due to multiple reflections between the mixer and the OMT, feed horn, and vertex of the subreflector. But it does not isolate image frequency signal components emerging from the input of the mixer which, in SIS mixers, can be substantial and can degrade the image rejection if there are reflections from the input components (OMT, feed horn, subreflector).

If a 180° input hybrid were used, as in Fig. 4, the undesired signal-to-image conversion products would be isolated from the input of the receiver, but the desirable well-matched input would be relinquished.

Using a balanced mixer with a 90° hybrid gives both good input match and good isolation of the undesired signal-to-image conversion products from the input, and also eliminates LO sideband noise from the IF output, but of course does not give sideband separation.

The ideal front end would be a balanced sideband-separating mixer, in which a 90° input hybrid feeds two balanced mixers, each of which has 90° hybrid. This would have all the virtues listed in Table 1 except that LO leakage would not be isolated from the receiver input. However LO leakage from the receiver input is unlikely to be a serious concern with SIS mixers which are relatively insensitive to LO power level under normal operating conditions. Specific advantages include:

–> matched input,
–> signal-to-image conversion is isolated from the input,
–> Down-converted LO sideband noise is isolated from the mixer output,
–> noise from the input hybrid termination is isolated from mixer output.

2. IF amplifiers

The current ALMA Band 6 receivers have a nominal IF band of 4-12 GHz. Typical SSB noise temperatures are between 40 and 60 K over a 6-10 GHz IF band, but increase at the IF band edges to 60-100 K at 4 GHz and over 60 K above 11 GHz. The very low SSB noise temperatures are facilitated by connecting the IF preamplifiers directly to the mixer block with no intervening lossy IF isolator.

Recently, Low-Noise Factory has produced cryogenic MMIC amplifiers with gain and noise comparable to those of the current NRAO Band-6 amplifiers, but with much flatter characteristics over a 3-13 GHz IF band. Using these LNF amplifiers as direct replacements for the standard Band-6 preamps has given excellent noise and image rejection, as shown in Figs. 5 and 6. The variation of the noise temperature across the IF band is due to the interaction between the mixer and the preamplifier, which also results in the variation in the mixer-preamp gain across the IF band, as shown in Fig. 7.

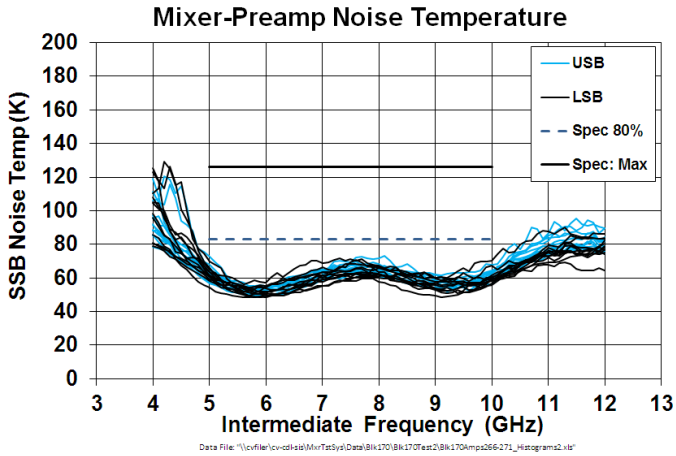

Fig. 5. SSB noise temperature of an experimental Band-6 mixer-preamp using LNF preamps.

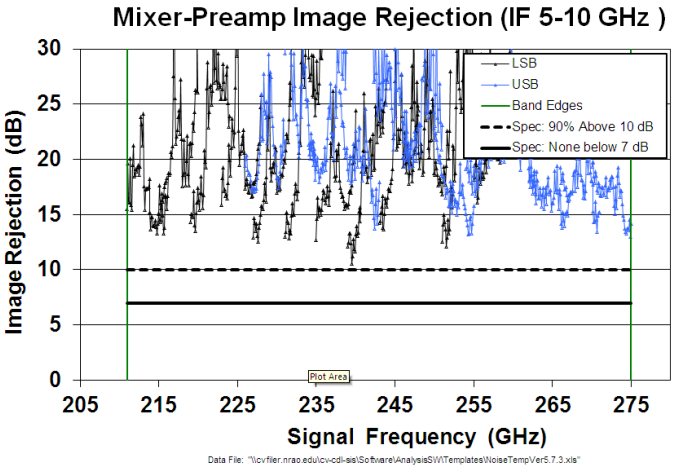

Fig. 6. Image rejection of an experimental Band-6 mixer-preamp using LNF preamps.

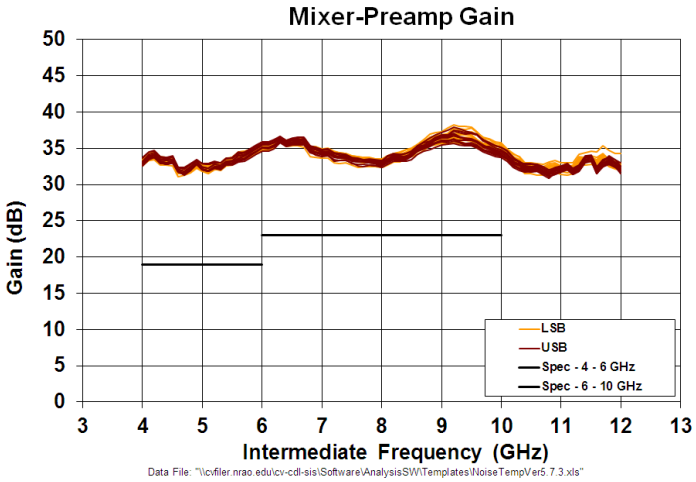

Fig. 7. Gain vs intermediate frequency for the experimental Band-6 mixer-preamp with LNF preamps.

Integrated Balanced IF amplifiers:

To improve the gain and noise flatness across the full IF band it is necessary to eliminate the interaction between the output of the mixer and the input of the preamp. This is done in some ALMA receivers using ferrite isolators, but these add significant loss – as much as 1 dB for a 4-12 GHz isolator – which results in a significant increase in receiver noise. Also, isolators are relatively large components, and the four required for a sideband-separating mixer receiver add to the congestion in the already cramped 4-K section of the receiver cartridge.

A better solution for the next generation of ALMA receivers will be to use balanced amplifiers. A balanced amplifier consists of two identical amplifiers in parallel, connected at their inputs to a quadrature hybrid and at their outputs to a second quadrature hybrid. A signal entering the input hybrid is coupled to the amplifiers with a 90° phase difference. The amplified signals emerging from the two amplifiers are combined in the second hybrid from which they emerge in phase from the same port. Signals reflected from the

(generally poorly matched) inputs of the elemental amplifiers are combined in the input hybrid and emerge from its fourth port which is terminated in a cold load. The noise analysis of a balanced amplifier is explained in [1].

Fig. 8 shows a photograph of a balanced amplifier using two Low-Noise Factory amplifiers and two MAC-Technology cryogenic quadrature hybrids. Unfortunately, the assembly is clearly too large to use in an ALMA dual-polarization receiver cartridge (which would require four such amplifiers). The proposed alternative, shown in Fig. 9, uses superconducting hybrids, which can be made on a quartz chip approximately 3 x 1 x 0.25 mm thick, in a single metal housing with two LNF amplifier chips and a standard NRAO SIS bias chip (2.8 x 1.3 mm). The complete balanced amplifier will be approximately the same size as the present Band-6 preamplifier.

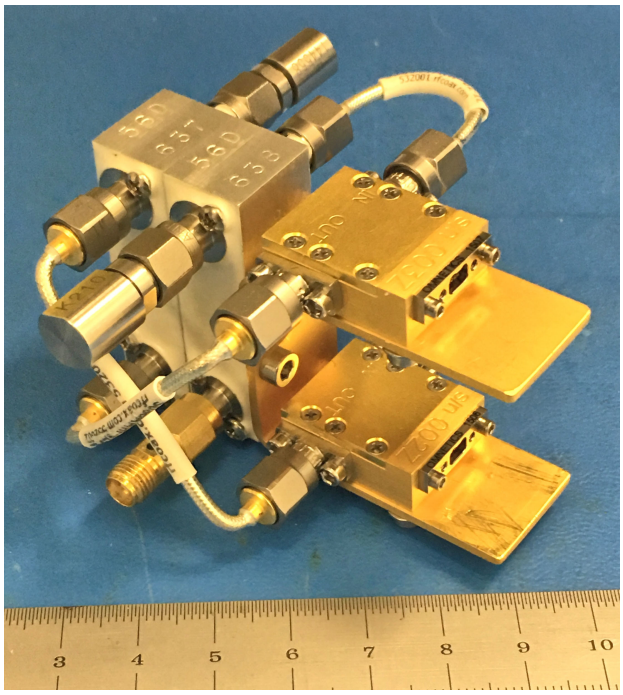

Fig. 8. Photograph of a balanced 4-12 GHz amplifier using discrete amplifiers (on the right) and hybrids (aluminum, on the left). The ruler indicates cm.

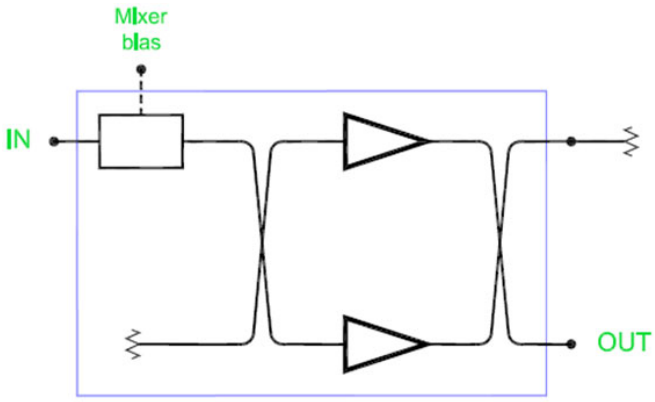

Fig. 9. Configuration of the balanced 4-12 GHz amplifier with two superconducting hybrids, two MMIC amplifier chips, and an SIS mixer bias-T integrated into a single housing.

Superconducting 4-12 GHz 90 ° hybrid:
The proposed integrated balanced amplifiers will need superconducting hybrids. The design of a superconducting 4-12 GHz 90 ° hybrid is almost complete. It remains to adjust the design to the dielectric layer properties currently being measured on test circuits at UVML (UVA Microfabrication Laboratory). Fig. 10 shows the 4-K test dewar we have assembled for measuring the hybrids.

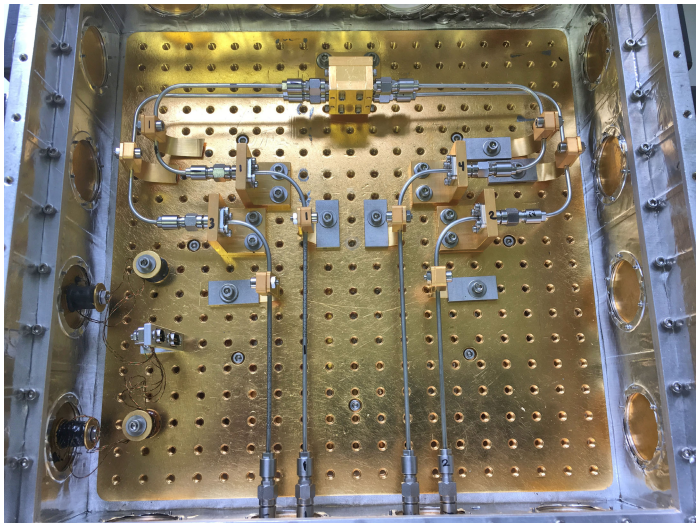

Fig. 10. Photograph of the hybrid test dewar. The 4-K cold plate is approximately 10" square.

3. Choice of IF band

It has been suggested that a future upgrade of ALMA receivers might benefit from changing the IF band from the current 4-12 GHz to something higher and wider. This would avoid the LO sideband noise which degrades the receiver noise temperatures significantly when operating at low IFs (around 4 to 5 GHz), and a wider IF band would hold the possibility of observing a greater variety of spectral lines simultaneously.

We have explored the consequences of changing to other IF bands using a list of spectral lines of general interest, and typical results are summarized in Figs. 11(a)-(c). These figures are from a spreadsheet in which the upper and lower IF limits can be entered in the box near the top (IF1 and IF2), and the IFs for the observable molecules appear in red – negative numbers correspond to lower sideband IFs, positive to upper sideband. The columns correspond to the LO frequencies in steps of 2.5 GHz.

There is disagreement as to whether it is necessary to observe the 220 GHz and 230 GHz CO lines simultaneously, but as simultaneous CO observation was one of the science drivers for selecting the IF band during the original design of the Band-6 receivers, we shall assume that requirement is still in place. It is clear from Fig. 11(a) that to observe the 220 and 230 GHz CO lines simultaneously in the lower respectively upper sideband, the lower end of the IF band can not be substantially below 4 GHz. Fig. 11(b) shows that by increasing the IF band from 4-12 GHz to 6-18 GHz (also a 3:1 frequency span) both CO lines can be observed in the lower sideband. Furthermore, as the IF system may be simplified by using an octave bandwidth (e.g., a ferrite isolator covering an octave is smaller and has lower loss than a 3:1 design), we also looked at the lowest octave IF band which could accommodate both CO lines simultaneously in the same sideband. The result, for a 13-26 GHz IF, is shown in Fig. 11(c).

As the input of the IF amplifier is the point of lowest signal level in the whole system, the noise temperature of the IF amplifier is of paramount importance. The contribution to the receiver noise temperature of a 1K increase in T_{IF} would typically be 3-10 K SSB, depending on the conversion loss of the mixer.

Moreover, as Marian Pospieszalski has pointed out [2][3]: (i) above a few GHz, the noise temperature of IF amplifiers is generally greater at higher frequencies, and (ii) the noise temperature of a wideband amplifier tends to be set by the high end of the band. Therefore, going to a substantially higher IF as suggested above can be expected to have an unacceptable receiver noise penalty.

(a)

IF1 4 GHz
IF2 12 GHz

Species	Chemical Name	Freq-GHz	LO GHz	220.0	222.5	225.0	227.5	230.0	232.5	235.0	237.5	240.0	242.5	245.0	247.5	250.0	252.5	255.0	257.5	260.0	262.5	265.0
HC3N	Cyanoacetylene	200.13539		-19.9																		
13C18O	CarbonMonoxide	209.41914		-10.6																		
H2CO	Formaldehyde	211.21147		-8.8	-11.3																	
13C17O	CarbonMonoxide	214.57387		-5.4	-7.9	-10.4																
DCO+	Formylium	216.11258			-6.4	-8.9	-11.4															
DCN	HydrogenCyanide	217.23854			-5.3	-7.8	-10.3															
H2CO	Formaldehyde	218.22219			-4.3	-6.8	-9.3	-11.8														
H2CO	Formaldehyde	218.76007				-6.2	-8.7	-11.2														
C18O	CarbonMonoxide	219.56035				-5.4	-7.9	-10.4														
13CO	CarbonMonoxide	220.39868				-4.6	-7.1	-9.6														
C17O	CarbonMonoxide	224.71419		4.7				-5.3	-7.8	-10.3												
H2CO	Formaldehyde	225.69778		5.7				-4.3	-6.8	-9.3	-11.8											
HC3N	Cyanoacetylene	227.41890		7.4	4.9				-5.1	-7.6	-10.1											
CO	CarbonMonoxide	230.53800		10.5	8.0	5.5				-4.5	-7.0	-9.5	-12.0									
CH3OH	Methanol	234.68339				9.7	7.2	4.7				-5.3	-7.8	-10.3								
HC3N	Cyanoacetylene	236.51279				11.5	9.0	6.5	4.0				-6.0	-8.5	-11.0							
CH3OH	Methanol	239.74625						9.7	7.2	4.7				-5.3	-7.8	-10.3						
C34S	CarbonMonosulfide	241.01609						11.0	8.5	6.0					-6.5	-9.0	-11.5					
CS	CarbonMonosulfide	244.93556								9.9	7.4	4.9				-5.1	-7.6	-10.1				
SO	SulfurMonoxide	246.40459								11.4	8.9	6.4					-6.1	-8.6	-11.1			
HC3N	Cyanoacetylene	254.69950												9.7	7.2	4.7				-5.3	-7.8	-10.3
H13CN	HydrogenCyanide	259.01180													11.5	9.0	6.5	4.0				-6.0
HN13C	HydrogenIsocyanide	261.26339														11.3	8.8	6.3				
HC3N	Cyanoacetylene	263.79231															11.3	8.8	6.3			
HCN	HydrogenCyanide	265.88643																10.9	8.4	5.9		
HCO+	Formylium	267.55763																	10.1	7.6	5.1	
CH3OH	Methanol	269.67951																		9.7	7.2	4.7
HNC	HydrogenIsocyanide	271.98114																		12.0	9.5	7.0
13CS	CarbonMonosulfide	277.45541																				12.5

Fig. 11. Band 6 line coverage with different IF bands. (a) 4−12 GHz. (b) 6-18 GHz. (c) 13-26 GHz. The columns correspond to the LO frequencies in steps of 2.5 GHz. The IFs for the observable molecules appear in red – negative numbers correspond to lower sideband IFs, positive to upper sideband. ***Fig. 11 continued on next page....***

(b)

IF1 6 GHz
IF2 18 GHz

Species	Chemical Name	Freq-GHz	LO GHz	220.0	222.5	225.0	227.5	230.0	232.5	235.0	237.5	240.0	242.5	245.0	247.5	250.0	252.5	255.0	257.5	260.0	262.5	265.0
HC3N	Cyanoacetylene	200.13539		-19.9																		
13C18O	CarbonMonoxide	209.41914		-10.6	-13.1	-15.6																
H2CO	Formaldehyde	211.21147		-8.8	-11.3	-13.8	-16.3															
13C17O	CarbonMonoxide	214.57387			-7.9	-10.4	-12.9	-15.4	-17.9													
DCO+	Formylium	216.11258			-6.4	-8.9	-11.4	-13.9	-16.4													
DCN	HydrogenCyanide	217.23854				-7.8	-10.3	-12.8	-15.3	-17.8												
H2CO	Formaldehyde	218.22219				-6.8	-9.3	-11.8	-14.3	-16.8												
H2CO	Formaldehyde	218.76007				-6.2	-8.7	-11.2	-13.7	-16.2												
C18O	CarbonMonoxide	219.56035					-7.9	-10.4	-12.9	-15.4	-17.9											
13CO	CarbonMonoxide	220.39868					-7.1	-9.6	-12.1	-14.6	-17.1											
C17O	CarbonMonoxide	224.71419							-7.8	-10.3	-12.8	-15.3	-17.8									
H2CO	Formaldehyde	225.69778							-6.8	-9.3	-11.8	-14.3	-16.8									
HC3N	Cyanoacetylene	227.41890		7.4						-7.6	-10.1	-12.6	-15.1	-17.6								
CO	CarbonMonoxide	230.53800		10.5	8.0						-7.0	-9.5	-12.0	-14.5	-17.0							
CH3OH	Methanol	234.68339		14.7	12.2	9.7	7.2						-7.8	-10.3	-12.8	-15.3	-17.8					
HC3N	Cyanoacetylene	236.51279		16.5	14.0	11.5	9.0	6.5						-8.5	-11.0	-13.5	-16.0					
CH3OH	Methanol	239.74625			17.2	14.7	12.2	9.7	7.2						-7.8	-10.3	-12.8	-15.3	-17.8			
C34S	CarbonMonosulfide	241.01609				16.0	13.5	11.0	8.5	6.0					-6.5	-9.0	-11.5	-14.0	-16.5			
CS	CarbonMonosulfide	244.93556					17.4	14.9	12.4	9.9	7.4						-7.6	-10.1	-12.6	-15.1	-17.6	
SO	SulfurMonoxide	246.40459						16.4	13.9	11.4	8.9	6.4					-6.1	-8.6	-11.1	-13.6	-16.1	
HC3N	Cyanoacetylene	254.69950									17.2	14.7	12.2	9.7	7.2						-7.8	-10.3
H13CN	HydrogenCyanide	259.01180											16.5	14.0	11.5	9.0	6.5					
HN13C	HydrogenIsocyanide	261.26339												16.3	13.8	11.3	8.8	6.3				
HC3N	Cyanoacetylene	263.79231													16.3	13.8	11.3	8.8	6.3			
HCN	HydrogenCyanide	265.88643														15.9	13.4	10.9	8.4			
HCO+	Formylium	267.55763														17.6	15.1	12.6	10.1	7.6		
CH3OH	Methanol	269.67951															17.2	14.7	12.2	9.7	7.2	
HNC	HydrogenIsocyanide	271.98114																17.0	14.5	12.0	9.5	7.0
13CS	CarbonMonosulfide	277.45541																		17.5	15.0	12.5

(c)

IF1 13 GHz
IF2 26 GHz

Species	Chemical Name	Freq-GHz	LO GHz	220.0	222.5	225.0	227.5	230.0	232.5	235.0	237.5	240.0	242.5	245.0	247.5	250.0	252.5	255.0	257.5	260.0	262.5	265.0
HC3N	Cyanoacetylene	200.13539		-19.9	-22.4	-24.9																
13C18O	CarbonMonoxide	209.41914			-13.1	-15.6	-18.1	-20.6	-23.1	-25.6												
H2CO	Formaldehyde	211.21147				-13.8	-16.3	-18.8	-21.3	-23.8												
13C17O	CarbonMonoxide	214.57387						-15.4	-17.9	-20.4	-22.9	-25.4										
DCO+	Formylium	216.11258						-13.9	-16.4	-18.9	-21.4	-23.9										
DCN	HydrogenCyanide	217.23854							-15.3	-17.8	-20.3	-22.8	-25.3									
H2CO	Formaldehyde	218.22219							-14.3	-16.8	-19.3	-21.8	-24.3									
H2CO	Formaldehyde	218.76007							-13.7	-16.2	-18.7	-21.2	-23.7									
C18O	CarbonMonoxide	219.56035								-15.4	-17.9	-20.4	-22.9	-25.4								
13CO	CarbonMonoxide	220.39868								-14.6	-17.1	-19.6	-22.1	-24.6								
C17O	CarbonMonoxide	224.71419										-15.3	-17.8	-20.3	-22.8	-25.3						
H2CO	Formaldehyde	225.69778										-14.3	-16.8	-19.3	-21.8	-24.3						
HC3N	Cyanoacetylene	227.41890											-15.1	-17.6	-20.1	-22.6	-25.1					
CO	CarbonMonoxide	230.53800												-14.5	-17.0	-19.5	-22.0	-24.5				
CH3OH	Methanol	234.68339		14.7												-15.3	-17.8	-20.3	-22.8	-25.3		
HC3N	Cyanoacetylene	236.51279		16.5	14.0											-13.5	-16.0	-18.5	-21.0	-23.5	-26.0	
CH3OH	Methanol	239.74625		19.7	17.2	14.7												-15.3	-17.8	-20.3	-22.8	-25.3
C34S	CarbonMonosulfide	241.01609		21.0	18.5	16.0	13.5											-14.0	-16.5	-19.0	-21.5	-24.0
CS	CarbonMonosulfide	244.93556		24.9	22.4	19.9	17.4	14.9												-15.1	-17.6	-20.1
SO	SulfurMonoxide	246.40459			23.9	21.4	18.9	16.4	13.9											-13.6	-16.1	-18.6
HC3N	Cyanoacetylene	254.69950						24.7	22.2	19.7	17.2	14.7										
H13CN	HydrogenCyanide	259.01180								24.0	21.5	19.0	16.5	14.0								
HN13C	HydrogenIsocyanide	261.26339									23.8	21.3	18.8	16.3	13.8							
HC3N	Cyanoacetylene	263.79231										23.8	21.3	18.8	16.3	13.8						
HCN	HydrogenCyanide	265.88643										25.9	23.4	20.9	18.4	15.9	13.4					
HCO+	Formylium	267.55763											25.1	22.6	20.1	17.6	15.1					
CH3OH	Methanol	269.67951												24.7	22.2	19.7	17.2	14.7				
HNC	HydrogenIsocyanide	271.98114													24.5	22.0	19.5	17.0	14.5			
13CS	CarbonMonosulfide	277.45541															25.0	22.5	20.0	17.5	15.0	

Fig. 11 (continued). Band 6 line coverage with different IF bands. (a) 4–12 GHz. (b) 6-18 GHz. (c) 13-26 GHz. The columns correspond to the LO frequencies in steps of 2.5 GHz. The IFs for the observable molecules appear in red – negative numbers correspond to lower sideband IFs, positive to upper sideband.

4. SIS mixers with increased RF bandwidth

Fig. 12 shows the average noise temperature of the ALMA Band-6 receivers, at an LO frequency of 225 GHz, across the extended (4-12 GHz) IF band. The variation has three causes: (i) interaction between the mixer and the preamplifier, which accounts for the periodic component; (ii) excess LO sideband noise, mainly below 6 GHz; and (iii) the inherent RF bandwidth of the mixer itself. As described above, the interaction between the mixer and the preamplifier can be eliminated by using balanced IF amplifiers, and the LO sideband noise can be reduced by using balanced component mixers in the overall sideband-separating mixer. The RF bandwidth of the mixer is limited by the capacitance of the SIS junction(s) and the series inductance of the junction circuit, as explained in detail in [4]. The red curve in Fig. 13 shows how the complex embedding impedance Z_e seen by the SIS junctions varies with frequency across Band 6. With lower capacitance SIS junctions in a redesigned mixer circuit it is possible to wrap the Z_e locus more tightly and achieve a wider, flatter frequency response.

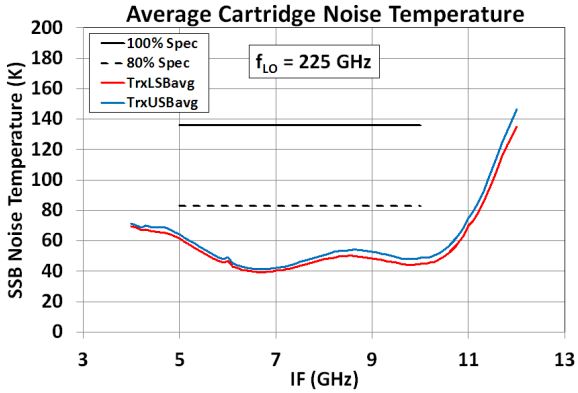

Fig. 12. The average noise temperature of the ALMA Band-6 receivers across the extended (4-12 GHz) IF band. The LO is at 225 GHz.

To reduce the series inductance, we have demonstrated a new, low inductance, circuit for SIS mixers using series arrays of junctions [5], and the

junction capacitance can be reduced by using junctions with higher critical current density.

To reduce the junction capacitance while maintaining the same junction conductance, the junction area can be reduced while increasing the critical current density J_C. The current Band-6 mixers use Nb/Al-AlOx/Al SIS junctions, whose I(V) characteristics deteriorate as J_C is increased beyond ~5,000 A/cm^2 but Nb/Al-AlN/Al SIS junctions allow a substantially higher J_C before the I(V) quality deteriorates. Fig. 14 shows I(V) characteristics of Band-6 mixers which are identical except that the left curve is for an AlOx tunnel barrier and the right curve is for an AlN barrier. Both have J_C ~ 5,200 A/cm^2. Both characteristics are of excellent quality, but the AlN barrier has a slightly higher gap voltage and a more abrupt current rise.

Having established that mixers with AlN tunnel barriers are at least as good as the current ALMA mixers with AlOx barriers, the next step will be to modify the RF circuit of the Band-6 mixer to use Nb/Al-AlN/Nb junctions with higher J_C and lower capacitance, thereby achieving a flatter RF response. Mixers with Nb/Al-AlN/Nb junctions have recently been fabricated at UVML and are currently being evaluated in the CDL.

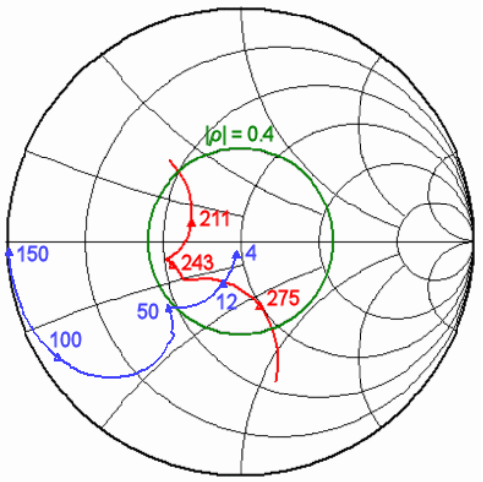

Fig 13. Complex embedding impedance Z_e seen by the current Band 6 SIS junctions as a function of frequency across Band 6. Red: RF Blue: IF.

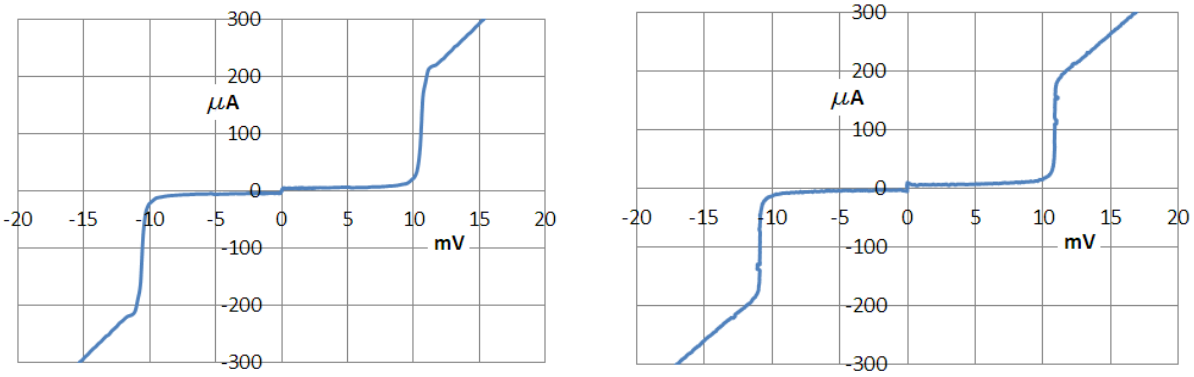

Fig. 14. I(V) characteristics. Left: Typical Band-6 mixer with Nb/Al-AlOx/Nb junctions. Right: Developmental Band 6 mixer with Nb/Al-AlN/Nb junctions. Both have J_C ~ 5,200 A/cm^2.

5. Conclusion

This study has laid the ground work for the next generation of ALMA Band-6 SIS receivers. The properties of balanced sideband-separating mixers have been examined in detail, and future SIS receivers should be made in this configuration if the additional complexity is acceptable – that will be determined in the next phase of development. The possible benefits of changing to a higher and wider IF have been studied, with the conclusion that there would be no substantial advantage in departing from the current 4-12 GHz band. New mixers, using Nb/Al-AlN/Nb SIS junctions, will have flatter characteristics across the full 211-275 GHz RF band, and balanced IF amplifiers will give receiver gain and noise temperature which are flat across the 4-12 GHz IF band. With chip-size superconducting quadrature hybrids and MMIC amplifier chips, these balanced IF amplifiers will not be substantially larger than the current ALMA IF amplifiers, and so will fit in the existing receiver cartridges. Their power dissipation will be comparable to that of the present amplifiers.

Appendix 1: Input Characteristics of Balanced and Sideband-Separating Mixers

The input characteristics of balanced and sideband-separating mixers with quadrature and 180° input hybrids are examined. Like the balanced amplifier, balanced and sideband-separating mixers using a quadrature input hybrid are inherently well matched. The levels of the signals emerging from the input port at the image and LO frequencies are also important in some applications, as are the down-converted local oscillator sideband noise and the thermal noise contribution of the fourth-port termination on the input hybrid. These depend on the mixer configuration.

INTRODUCTION

First described by Engelbrecht and Kurokawa in 1965 [6], the balanced amplifier has long been known for its inherently good input match. This is due to the quadrature hybrid at the input which phases the signals reflected back towards the source from the (identical) elemental amplifiers, so they cancel. For the same reason, the input of a balanced or sideband-separating mixer is inherently well matched when the input power divider is a quadrature hybrid, although this does not appear to be recognized in the literature.

The choice of input hybrid type also affects other characteristics of balanced and sideband-separating mixers. In addition to reflecting part of the incident signal power, most mixers convert some of the incident signal power from the signal frequency f_s to the image frequency $f_i = |f_s - f_{LO}|$. In a sideband-separating mixer, this image power emerging from the input port of the mixer can spoil the image rejection if it is partially reflected back into the mixer by a poorly matched source. This can be particularly significant in millimeter-wave radio astronomy receivers using superconductor-insulator-superconductor (SIS) tunnel junction mixers which can have substantial signal-to-image conversion [7].

Leakage of LO power from the input of a balanced or sideband-separating mixer can be undesirable when the signal source is not matched at the LO frequency. Then LO power reflected from the signal source back into the mixer to can spoil the balance of the mixer.

Thermal noise from the termination of the fourth port of the input hybrid or LO power splitter can contribute to the IF output noise of balanced and sideband-separating mixers.

These effects are considered for balanced and sideband-separating mixers of the four basic types depicted in Figs. 1-4. All have input hybrids, either quadrature or 180°. Quadrature hybrids can be of the coupled transmission line or branch-line types, and 180° hybrids can use a magic-T, Wilkinson power divider, rat-race, or a simple transformer. In practice, 0° or 180° three-port power splitters are sometimes used in place of 180° hybrids, but these can lead to degradation of mixer performance due to reflection of even- or odd-mode signal components which would be terminated in the fourth-port load of a full four-port hybrid.

The balanced mixer of Fig. 1(a) is frequently simplified by connecting the LO to the fourth port of the input quadrature hybrid, as shown in Fig. 1(b); Figs 1(a) and 1(b) are in most respects equivalent. Likewise, the balanced mixer of Fig. 2(b) is similar to that of Fig. 2(a). *In both cases the simpler configuration has the advantage that it requires less LO power.*

ANALYSIS

In the following analysis it is assumed that the component mixers, M1 and M2, are identical and have an input reflection coefficient ρ at the signal frequency f_s. For quadrature hybrids the coupling factors (*i.e.*, S-parameters) are $t = 1/\sqrt{2}$ and $q = \left(1/\sqrt{2}\right)\exp\left(-j\pi/2\right)$, and for 180° hybrids, the coupling factors are $\pm 1/\sqrt{2}$. The following phase relations for the elemental mixers (simple single-ended double-sideband mixers) are used:

(i) A phase change $\delta\theta$ in an upper sideband (USB: $f_{LO} + f_{IF}$) input signal produces a phase change $\delta\theta$ in the IF output signal.

(ii) A phase change $\delta\theta$ in a lower sideband (LSB: $f_{LO} - f_{IF}$) input signal produces a phase change $-\delta\theta$ in the IF output signal.
(iii) A phase change $\delta\theta$ in the LO produces a phase change $-\delta\theta$ in the IF output signal generated by an USB input signal.
(iv) A phase change $\delta\theta$ in the LO produces a phase change $\delta\theta$ in the IF output signal generated by an LSB input signal.
(v) A phase change $\delta\theta$ in the LO produces a phase change $2\delta\theta$ in the image frequency ($f_{LO} - f_{IF}$) or ($f_{LO} + f_{IF}$) signal produced in the mixer by a USB or LSB input signal, resp.

A. Balanced mixer with quadrature hybrid input

1) Input reflection

Fig. A1 shows the components $aq\rho$ and $at\rho$ of input signal a reflected from the component mixers M1 and M2 in a balanced mixer with a quadrature hybrid at its input. Since $t^2 + q^2 = 0$, it is clear that the input is matched regardless of the reflection coefficients (assumed equal) of the individual mixers. The signal power reflected from the component mixers is all delivered to the load R_D (or, in the case of the more common configuration of Fig. 1(b), to the LO port).

2) Signal-to-image conversion

Fig. A2 shows the image frequency components, x_1 and x_2, produced at the component mixers M1 and M2 by input signal a in a balanced mixer with a quadrature hybrid at its input. Because of the quadrature phase relationship of the signal and LO in the two component mixers, $x_2 = x_1 \exp(-j\pi/2)$. The image frequency signal emerging from the signal port of the mixer is

$$x_1 t + x_2 q = x_1 \left[1 + \exp(-j\pi/2)\exp(-j\pi/2)\right]/\sqrt{2} = 0 .$$

Likewise, the image frequency signal emerging from the LO port is

$$x_1 q + x_2 t = x_1 \left[\exp(-j\pi/2) + \exp(-j\pi/2)\right]/\sqrt{2} = x_1 \sqrt{2} \exp(-j\pi/2) .$$

The emerging image-frequency power is thus all coupled to the resistor R_D, with none coupled to the input port of the mixer. In the case of the Fig. 1(b) configuration, the emerging image-frequency power is thus all coupled to the LO port.

3) LO leakage

Fig. A3 shows the components c_1 and c_2 of the LO power reflected from the component mixers M1 and M2 in a balanced mixer with a quadrature hybrid at its input. When the (identical) mixers are driven by equal LO powers, $c_1 = c_2 \exp(-j\pi/2)$. Then the power delivered to the load R_D is $c_1 q + c_2 t = 0$, and all the reflected LO power is delivered to the signal input port. If the signal source is not matched, part of the emerging LO power ($2\,cqt\rho_L$) is reflected back into the balanced mixer where it arrives at the elemental mixers and adds (vectorially) to the LO components ct and cq, spoiling the quadrature phasing and amplitude balance of the LO drive to the mixers. In the case of the Fig. 1(b) configuration, the LO port is matched.

4) Noise from the input and LO hybrid terminations, and LO sideband noise

Thermal noise from the input hybrid termination R_D is delivered to the Σ-termination on the IF hybrid, while noise from the fourth-port termination on the LO hybrid, attenuated by the LO coupler, is delivered to the IF outport port. As in all balanced mixers, LO sideband noise entering the mixer with the LO signal produces in-phase IF components at mixers M1 and M2, which are delivered to the termination R_Σ on the IF hybrid.

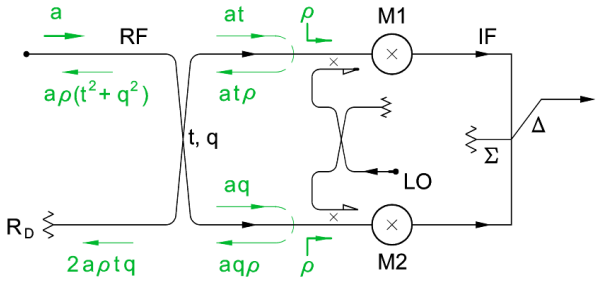

Fig. A1. Fig. 5. Input reflection for balanced mixer with a quadrature hybrid at its input.

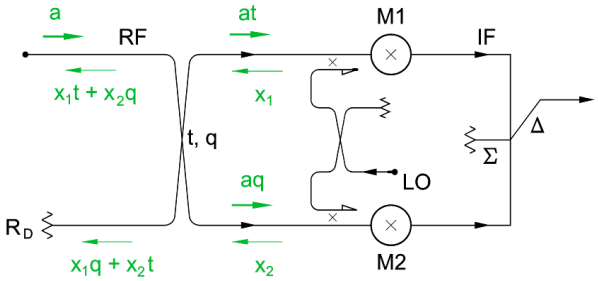

Fig. A2. Signal-to-image conversion for a balanced mixer with a quadrature hybrid at its input.

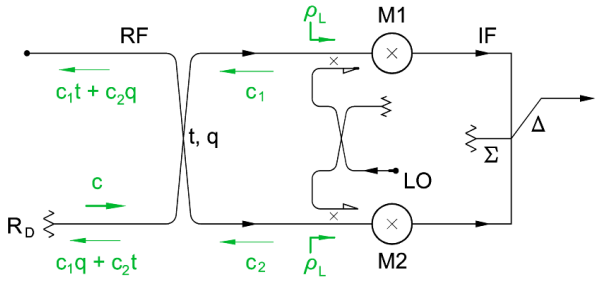

Fig. A3. LO Leakage for balanced mixer with a quadrature hybrid at its input.

B. Sideband-separating mixer with quadrature hybrid input

1) Input reflection

Fig. A4 shows the components $at\rho$ and $aq\rho$ of input signal a reflected from the component mixers M1 and M2 in a sideband-separating mixer with a quadrature hybrid at its input. Since $t^2 + q^2 = 0$, it is clear that the input is matched regardless of the reflection coefficients (assumed equal) of the component mixers. The signal power reflected from the component mixers is all delivered to the image termination R_{IM}.

2) Signal-to-image conversion

Fig. A5 shows the image frequency components, x_1 and x_2, produced by an input signal a at the component mixers M1 and M2 of a sideband-separating mixer with a quadrature hybrid at its input. Because the component mixers are driven in phase by the LO, and their input signals at and aq are in quadrature, the image signals emerging from M1 and M2 are also in quadrature, with $x_2 = x_1 \exp(j\pi/2)$. The image frequency signals coupled to the input port and image termination R_{IM} are therefore, respectively,

$$x_1 t + x_2 q = x_1\left[t + q\exp(j\pi/2)\right] = x_1\left[1 + \exp(j\pi/2)\exp(-j\pi/2)\right]/\sqrt{2} = \sqrt{2}x_1$$

and

$$x_1 q + x_2 t = x_1\left[q + t\exp(j\pi/2)\right] = x_1\left[\exp(-j\pi/2) + \exp(j\pi/2)\right]/\sqrt{2} = 0.$$

Hence all the image frequency power is delivered to the input port and none to the load R_{IM}.

3) LO leakage

Fig. A6 shows the components c_1 and c_2 of the LO power emerging from the component mixers M1 and M2 in a sideband-separating mixer with a quadrature hybrid at its input, when the component mixers M1 and M2 are identical. Since $c_1 = c_2$, the LO leakage coupled to both the input port and the image termination R_{IM} is

$$c_1(t+q) = c_1\left(1/\sqrt{2}\right)\left[1 + \exp(-j\pi/2)\right] = c_1\exp(-j\pi/4).$$

This is the same LO leakage power as would emerge from the input of a simple single-ended DSB mixer.

4) Noise from the input and LO hybrid terminations, and LO sideband noise

Thermal noise from the fourth-port termination R_{IM} on the input hybrid is down-converted to the USB and LSB outputs of the mixer; noise from the USB converts to the LSB IF port, while noise in the LSB converts to the USB IF port. Noise from the Δ-port termination of the LO hybrid is down-converted, attenuated by the LO coupler, and delivered equally to the USB and LSB IF ports of the mixer. Sideband noise accompanying the LO signal is likewise delivered to both IF ports.

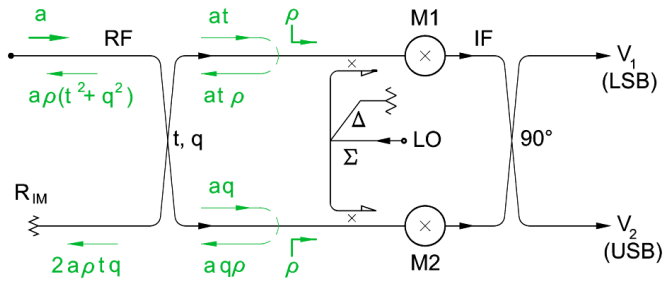

Fig. A4. Input reflection for a sideband-separating mixer with a quadrature hybrid at its input.

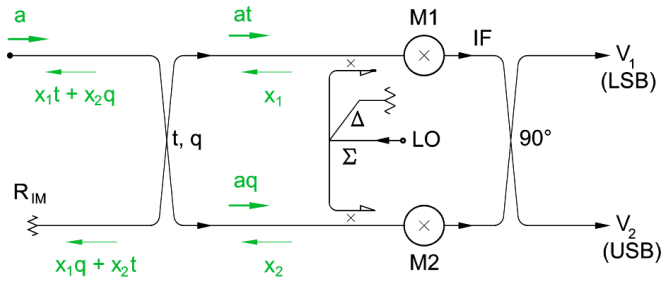

Fig. A5. Signal-to-image conversion for a sideband-separating mixer with a quadrature hybrid at its input.

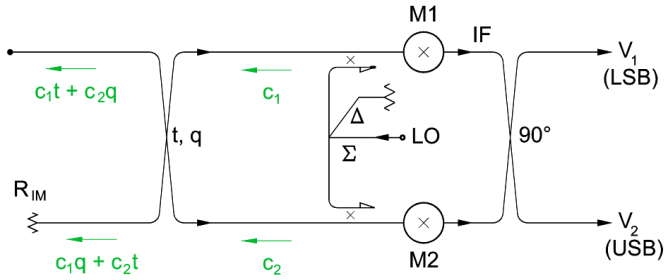

Fig. A6. LO leakage for a sideband-separating mixer with a quadrature hybrid at its input.

C. Balanced mixer with 180° hybrid input

1) Input reflection

Fig. A7 shows the components $a\rho/\sqrt{2}$ and $-a\rho/\sqrt{2}$ of input signal a reflected from the component mixers M1 and M2 in a balanced mixer with a 180° hybrid at its input. The hybrid combines these components to give a reflected signal $a\rho$ at the input port – the same as at the input of a simple single-ended mixer. No signal power is delivered to the Σ-port termination of the input hybrid.

2) Signal-to-image conversion

Fig. A8 shows the image frequency components, x_1 and x_2, produced by an input signal a at the component mixers M1 and M2 in a balanced mixer with a 180° hybrid at its input. At the component mixers, the incident signals are out of phase while the LO is in phase, so image signal $x_2 = -x_1$. The image signals add in the hybrid to give an outgoing image signal $x_1/\sqrt{2} + x_2/\sqrt{2} = \sqrt{2}\, x_1$ at the input of the mixer, the same as would emerge from the input of a simple single-ended mixer. No image-frequency power is delivered to the Σ-port termination of the input hybrid.

3) LO leakage

Fig. A9 shows the components c_1 and c_2 of the LO power emerging from the component mixers M1 and M2 in a balanced mixer with a 180° hybrid at its input. Because component mixers M1 and M2 are identical and driven in-phase by the LO, the LO signals emerging at their inputs are equal and in phase: $c_2 = c_1$. The LO power emerging from the input of the balanced mixer is $c_1/\sqrt{2} - c_2/\sqrt{2} = 0$. All the LO leakage power is delivered to the Σ-port termination of the input hybrid.

4) Noise from the input and LO hybrid terminations, and LO sideband noise

Thermal noise from the Σ-port termination of the input hybrid is down-converted to the Σ-port of the IF hybrid together with sideband noise from the LO source. Noise from the Δ-port termination of the LO hybrid is attenuated by the LO coupler and down-converted to the IF output.

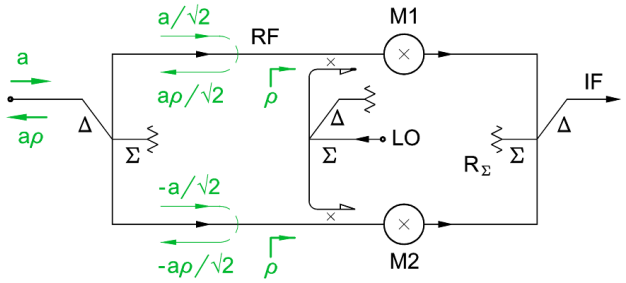

Fig. A7. Input reflection for a balanced mixer with a 180° hybrid at its input.

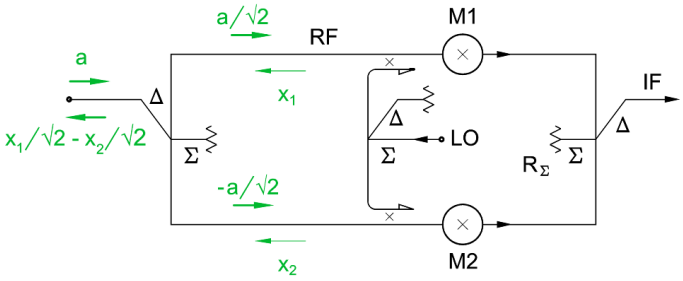

Fig. A8. Signal-to-image conversion for a balanced mixer with a 180° hybrid at its input.

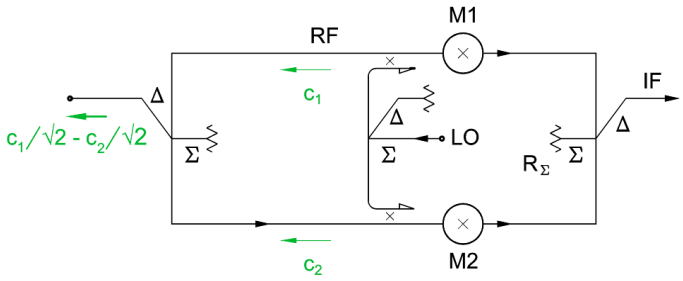

Fig. A9. LO leakage for a balanced mixer with a 180° hybrid at its input.

D. Sideband-separating mixer with 180° hybrid input

1) Input reflection

Fig. A10 shows the components $a\rho/\sqrt{2}$ of the input signal a reflected from the component mixers M1 and M2 in a sideband-separating mixer with a 180° hybrid at its input. The hybrid combines these components to give a reflected signal $a\rho$ at the input port – the same as at the input of a simple single-ended DSB mixer.

2) Signal-to-image conversion

Fig. A11 shows the image frequency components, x_1 and x_2, produced by an input signal a at the component mixers M1 and M2 in a sideband-separating mixer with a 180° hybrid at its input. At the component mixers, the incident signals $a/\sqrt{2}$ are in phase, while the LO signals are in quadrature. Hence $x_2 = -x_1$ and all the image power is delivered to the termination R_{IM} while none is coupled to the input.

3) LO leakage

Fig. A12 shows the components c_1 and c_2 of the LO power reflected from the component mixers M1 and M2 in a sideband-separating mixer with a 180° hybrid at its input. The LO is in quadrature at the component mixers, so $c_1 = c_2 \exp(-j\pi/2)$. The LO power emerging from M1 and M2 is therefore equally divided between the input port of the mixer and the termination R_{IM}.

4) Noise from the input and LO hybrid terminations, and LO sideband noise

Thermal noise from the Δ-port termination R_{IM} on the input hybrid is down-converted to the USB and LSB outputs of the mixer; noise in the USB converts to the LSB IF port, while noise in the LSB converts to the USB IF port. Noise from the Δ-port termination of the LO hybrid is attenuated by the LO coupler, down-converted, and delivered equally to the USB and LSB IF ports of the mixer. Sideband noise accompanying the LO signal is likewise delivered to both IF ports.

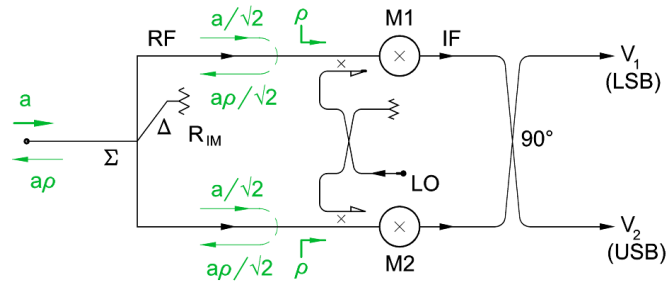

Fig. A10. Input reflection for a sideband-separating mixer with a 180° hybrid at its input.

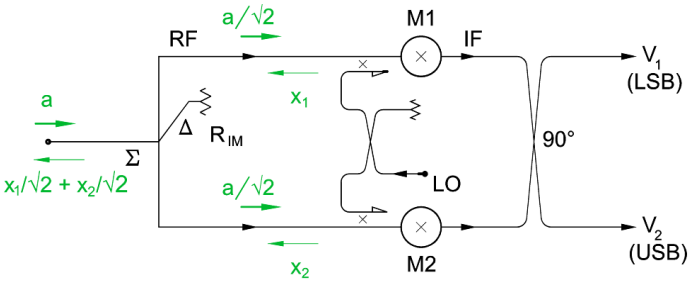

Fig. A11. Signal-to-image conversion for a sideband-separating mixer with a 180° hybrid at its input.

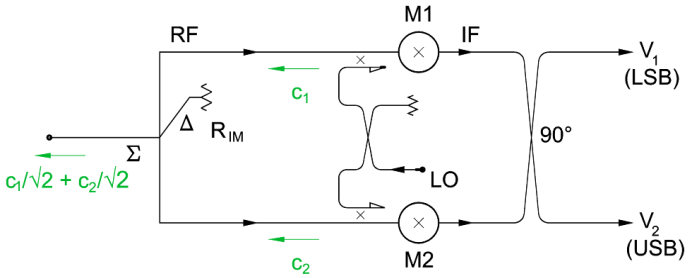

Fig. A12. LO leakage for a sideband-separating mixer with a 180° hybrid at its input.

REFERENCES

[1] A. R. Kerr, "On the Noise Properties of Balanced Amplifiers," *IEEE Microwave and Guided Wave Letters*, vol. 8, no. 11, pp. 390-392, Nov. 1998. http://ieeexplore.ieee.org/stamp/stamp.jsp?tp=&arnumber=736255

[2] M. W. Pospieszalski, "HFET's and Receivers for the Millimeter - Wave Array," MMA (now ALMA) Memo 67, 12 Aug 1991. http://library.nrao.edu/public/memos/alma/memo067.pdf

[3] M. W. Pospieszalski, "ALMA IF Amplifier Performance," NRAO internal memorandum, 9 Nov 1999.

[4] A. R. Kerr, "Some fundamental and practical limits on broadband matching to capacitive devices, and the implications for SIS mixer design," IEEE Trans. Microwave Theory Tech., vol. MTT-43, no. 1, pp. 2-13, Jan. 1995. http://ieeexplore.ieee.org/stamp/stamp.jsp?tp=&arnumber=363015

[5] See companion report on the development of second-generation mixers for ALMA Band 10.

[6] R. S. Engelbrecht and K. Kurokawa, "A wideband low noise L-band balanced transistor amplifier," Proc. IEEE, vol. 53, pp. 237–247, Mar. 1965. http://ieeexplore.ieee.org/stamp/stamp.jsp?tp=&arnumber=1445611

[7] A. R. Kerr, S.-K. Pan, S. M. X. Claude, P. Dindo, A. W. Lichtenberger, J. E. Effland and E. F. Lauria, "Development of the ALMA-North America Sideband-Separating SIS Mixers," IEEE Trans. Terahertz Science and Technology, v. 4, no. 2, pp. 201-212, Mar 2014. http://ieeexplore.ieee.org/stamp/stamp.jsp?tp=&arnumber=6740089